Tikrit Journal of Pure Science Vol. 31 (3) 2026

DOI:https://doi.org/10.25130/tjps.v31i3.1930

IRAQI Academic Scientific Journals

Tikrit Journal of Pure Science

ISSN: 1813 – 1662 (Print) --- E-ISSN: 2415 – 1726 (Online)

Journal Homepage: https://tjpsj.org/

Tikrit Journal of Pure Science

Study of Optical Properties of NiO and $Ni_{0.92}Zn_{0.08}O$ Thin Films Prepared by Pulsed Laser Deposition via Kramers–Kronig Analysis

Mustafa F. Hamad[1], Najat A. Dahham[2]

[1,2]Department of Physics, College of Science, University of Tikrit, Tikrit, Iraq

Received: 4 Mar. 2025 **Received in revised forum:** 17 May. 2025 **Accepted:** 22 May. 2025

Final Proofreading: 12 Jun. 2025 **Available online:** 25 Jun. 2026

ABSTRACT

NiO and $Ni_{0.92}Zn_{0.08}O$ thin films were deposited onto glass substrates using pulsed laser deposition in vacuum. The optical properties were investigated using the Kramers-Kronig relations, with the phase shift angle computed numerically in MATLAB. The results revealed noticeable variations in the optical behavior due to zinc doping, as confirmed by differences in the refractive indices: 2.52 and 2.57 at 630 nm for the undoped and doped films, respectively. Moreover, the optical band gap decreased from 3.51 to 3.39 eV, and the dielectric constant was also calculated. X-ray diffraction (XRD) analysis confirmed the polycrystalline nature of the prepared films, while field emission scanning electron microscopy (FESEM) images revealed a surface morphology characterized by nanoscale grains. Moreover, energy-dispersive X-ray spectroscopy (EDX) and Fourier-transform infrared (FTIR) spectroscopy were performed to verify the elemental composition and investigate the chemical bonding of both films.

Keywords: Kramers-Kronig Calculations, Linear Optical Properties, NiO Thin Films, PLD, Zn doping.

Name: Mustafa F. Hamad **E-mail:** mustafa.fayiq@st.tu.edu.iq

©2026 THIS IS AN OPEN ACCESS ARTICLE UNDER THE CC BY LICENSE http://creativecommons.org/licenses/by/4.0/

Tikrit Journal of Pure Science Vol. 31 (3) 2026

DOI:https://doi.org/10.25130/tjps.v31i3.1930

دراسة الخصائص البصرية لاغشية NiO و $Ni_{0.92}Zn_{0.08}O$ الرقيقة المحضرة باستخدام تقنية الترسيب بالليزر النبضي من خلال تحليل كرامرز–كرونيج

مصطفى فايق حمد[1]، نجاة احمد دحام[2]

[2,1]قسم الفيزياء، كلية العلوم، جامعة تكريت، تكريت، العراق

الملخص

تم ترسيب اغشية NiO و$Ni_{0.92}Zn_{0.08}O$ النانوية على قواعد من الزجاج باستخدام تقنية الترسيب بالليزر النبضي في الفراغ، تم دراسة الخواص البصرية من خلال علاقات كرامرز–كرونيج، حيث تم حساب زاوية انحراف الطور عدديا باستخدام برمجة ماتلاب. أظهرت النتائج اختلافا في السلوك البصري بسبب تأثير إضافة الخارصين وهذا ما أثبته الاختلاف في قيم معامل الانكسار حيث كانت القيم عند الطول الموجي 630 نانومتر تساوي 2.52 و2.57 للغشائين النقي والمشوب على التوالي. كما انخفضت قيمة فجوة الطاقة من 3.51 الى 3.39 الكترون–فولت. كما تم حساب قيم ثابت العزل الكهربائي. اكد فحص حيود الاشعة السينية الطبيعة متعددة التبلور للأغشية المحضرة واظهرت صور المجهر الالكتروني الماسح بالمجال سطوح الاغشية ذات الطبيعة الحبيبية بالمدى النانوي . فضلا عن ذلك اجري اختبار مطيافية طاقة تشتت الاشعة السينية وتحويلات فورريه للأشعة تحت الحمراء للتحقق من تكوين العناصر وطبيعة الاواصر في الاغشية المحضرة.

INTRODUCTION

Metal oxide-based thin films have attracted the attention of researchers due to their wide applications. Among these oxides, nickel oxide (NiO) stands out as a p-type metal oxide with a wide energy gap, owing to its important optical and electrical properties for optoelectronic applications. [(1)]. Doping with metals is one of the most effective methods for improving the properties of NiO thin films. Studies have been conducted on doping NiO with various materials, including Ag, Cu, Li, Al and Zn. [(2-5)]. Among the various impurities, Zn was chosen in this study due to its slight difference in ionic radius with Ni^{+2}, which facilitates its incorporation into the NiO lattice and results in structural and optical changes in the doped films. [(6)]. There are many methods for preparing NiO and $Ni_{0.92}Zn_{0.08}O$ thin films. In this study, pulsed laser deposition (PLD) was used, as it is known to produce high-quality thin films with good crystallinity.[(7)]. There are many studies on the optical properties of pure and Zn-doped NiO thin films. Still, studies using the Kramers-Kronig (K-K) relations are very limited, despite their use in films doped with other materials such as Ga-doped ZnO and In-doped CdO. [(8, 9)]. The K-K method is the most effective for accurately extracting optical parameters. Yet, only a few studies have adopted it, making this paper an important source for future research. Therefore, this study aims to prepare NiO and $Ni_{0.92}Zn_{0.08}O$ thin films by PLD and to determine their optical parameters using the K-K relations.

MATERIALS AND METHODS

NiO powder, obtained from (BDH Chemicals Ltd.), and Zn powder from the same source were employed in this study. 0.06 g of Zn was homogeneously blended with 1.94 g of NiO using an agate mortar for 10 minutes. Subsequently, two targets were prepared: one containing pristine NiO and the other containing Zn-doped NiO. The powders were compacted using a hydraulic press at 5 tons (equivalent to(~625 MPa) for 5 minutes, forming discs with a thickness of 0.4 cm and a diameter of 1 cm. Thereafter, the two samples were

DOI:https://doi.org/10.25130/tjps.v31i3.1930

placed in a clean vacuum chamber under a pressure of 10^{-3} mbar, with a glass substrate with a target-to-substrate distance of 3 cm. A commercially available Q-switched Nd: YAG laser system (Model: Portable Q-Switched Nd: YAG Laser, Beijing Sincoheren S&T Development Co., Ltd., China), with a wavelength of 1064 nm, a repetition rate of 6 Hz, and a source energy of 700 mJ, was employed. Finally, the deposited films were annealed at 400°C for 1 hour. Figure 1 summarizes the synthesis method.

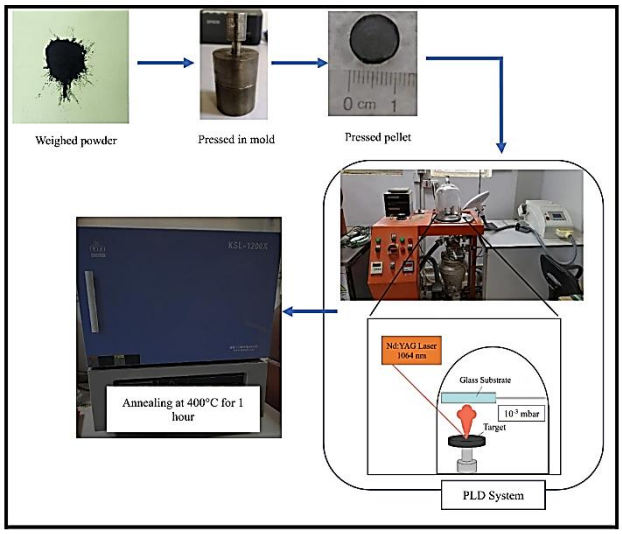

Fig. 1: Process flow for the synthesis of thin films using Pulsed Laser Deposition (PLD).

XRD analysis of the thin films was performed using a Philips PW-1730 with a wavelength of 1.5406 Å. Measurements were taken within a 2θ range from 10° to 80°. FESEM imaging of the surface morphology was carried out using a TESCAN MIRA3 with a magnification of 35,000x. Elemental analysis was conducted to confirm the absence of impurities in the films using an EDX spectrometer from (OXFORD INSTRUMENTS). FTIR spectroscopy was performed using a (FT/IR-4600 Type A) from (Jasco) to identify and analyze molecular functional groups based on infrared absorption. This instrument operates in the mid-infrared range from 400 cm^{-1} to 4000 cm^{-1}. Optical UV-Vis-NIR analysis was performed using a SP-8001 from Metertech Inc., a double-beam spectrometer with a bandwidth of <2 nm, to measure absorption and reflectance spectra.

RESULTS AND DISCUSSION

To verify the crystalline nature of the prepared films, XRD analysis was performed. The results confirmed the polycrystalline cubic structure of NiO, with distinct peaks appearing at 2θ positions of 37° and 43°, corresponding to the (111) and (200) crystal planes, respectively, as identified by matching with the standard reference pattern JCDPS Card No. 47-1049. A preferred growth orientation along the (200) plane was observed. Additionally, the $Ni_{0.92}Zn_{0.08}O$ film exhibited variations in peak intensity and a slight shift in the diffraction peak toward lower angles, indicating structural modifications in the NiO lattice upon Zn^{+2} incorporation. [10]. Notably, no additional phases related to Zn, its oxide, or any other impurities were detected in the prepared films. Figure 2 shows the XRD patterns of both thin films with the reference card.

DOI:https://doi.org/10.25130/tjps.v31i3.1930

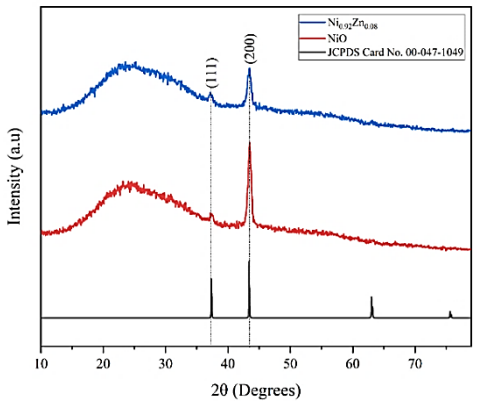

Fig. 2: XRD patterns of prepared thin films.

FESEM micrographs revealed that the prepared films exhibited a granular structure with nanometer-sized grains and scattered larger agglomerates in both films. The average grain size was approximately 38 nm for the pure NiO film and about 25 nm for the $Ni_{0.92}Zn_{0.08}O$ film, as estimated from the FESEM images. Additionally, no cracks or fractures were observed in the prepared films, as shown in Figure 3.

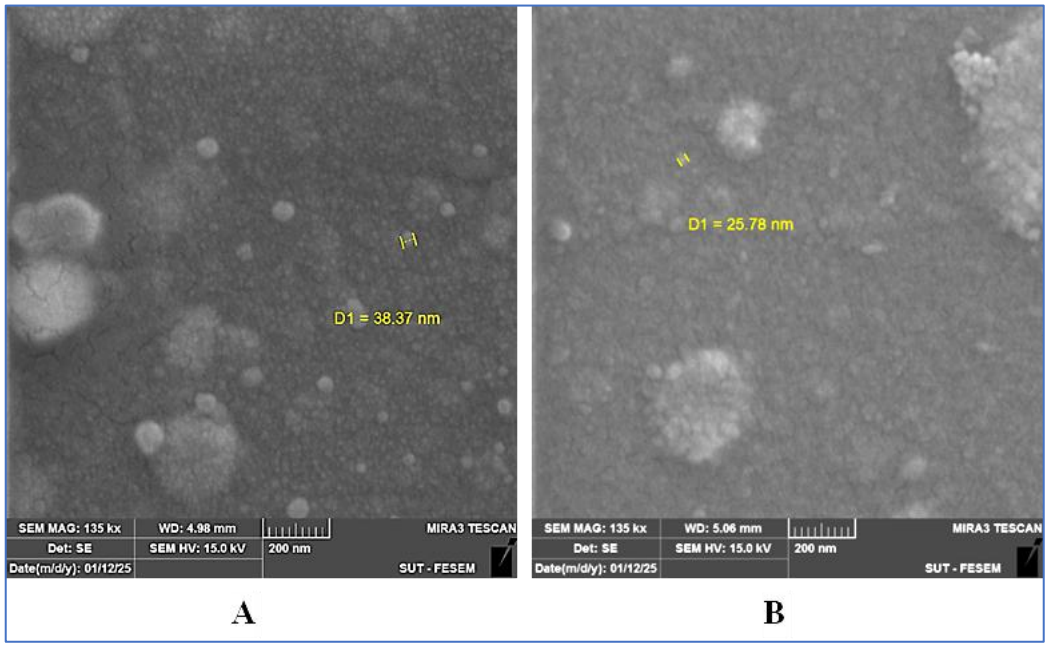

Fig. 3: FESEM micrographs of (a) pristine NiO, (b) $Ni_{0.92}Zn_{0.08}O$ fabricated thin films.

Elemental analysis by EDX confirmed the composition of the prepared films, revealing no detectable impurities. The atomic percentage of Zn in the doped film was 8%. The presence of Au in Figure 4 is due to the conductive coating layer applied to the sample before analysis.

FTIR analysis, as shown in Figure 5, showed strong agreement with XRD and EDX results, confirming the absence of any impurity-related bonds in the prepared films. A broad vibrational band characteristic of metal-oxygen bonding, i.e., Ni–O, was observed near 400 cm^{-1}[6]. In the Zn-doped film, a distinct peak emerged near 888 cm^{-1}, which was absent in the undoped counterpart. This peak is likely attributed to structural distortions introduced by Zn^{+2} incorporation into the NiO lattice, where Zn ions induce local lattice deformations, thereby activating vibrational modes not observed in the pure film.

DOI:https://doi.org/10.25130/tjps.v31i3.1930

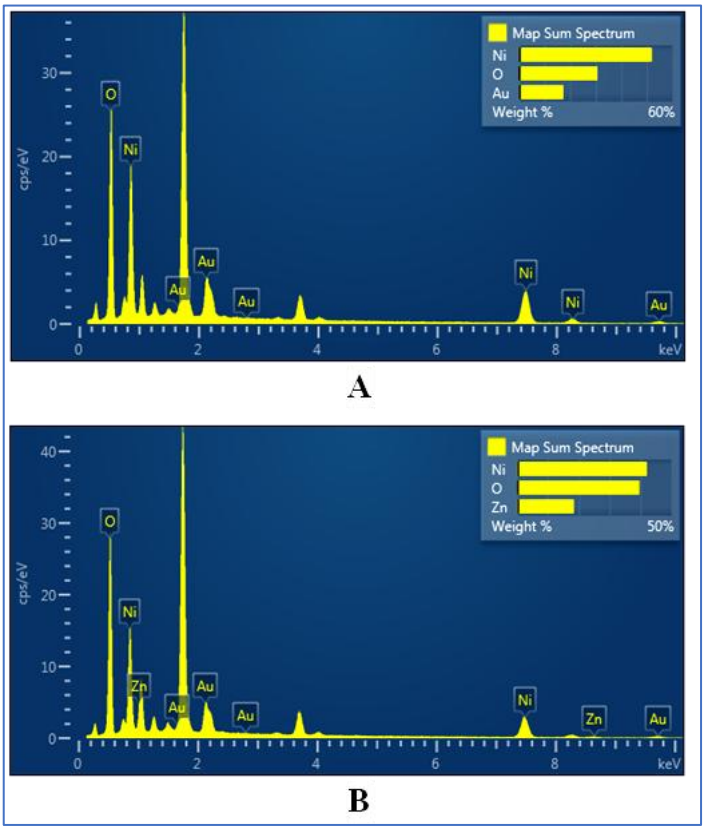

Fig. 4: EDX spectrum of (a) Undoped NiO, (b) $Ni_{0.92}Zn_{0.08}O$ thin films.

The adsorption of atmospheric moisture by the films resulted in weak peaks near 1500 cm-1, corresponding to H–O–H bonding vibrations.[11]. Furthermore, analyzing an open environment resulted in the emergence of a characteristic CO_2 peak near 2360 cm^{-1} [12]. Additionally, the weak peaks observed near 3770 cm^{-1} were attributed to O–H stretching vibrations. [13].

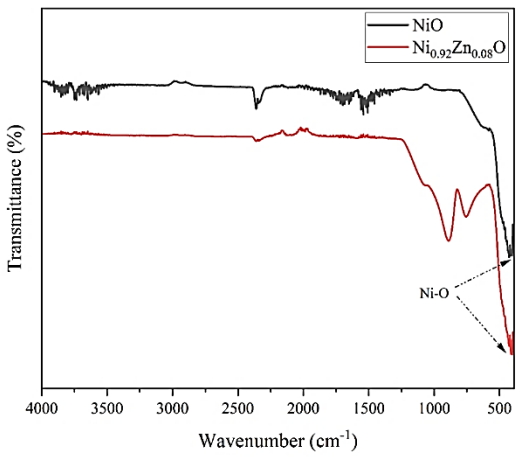

Fig. 5: FTIR spectrum of prepared thin films.

To investigate the optical behavior of the prepared films, optical properties were analyzed using a UV-Vis-NIR spectrophotometer. As shown in Figure 6a, the absorbance spectrum of the prepared films exhibits a distinct absorption peak in the ultraviolet region. Moreover, a slight redshift in the absorption peak is observed in the $Ni_{0.92}Zn_{0.08}O$ film, indicating electronic transitions and a reduction in its optical band gap.[14]. This observation is further corroborated by the Tauc plot, which allows determination of the optical band gap using the equation below. [15].

$$(\alpha h\nu)^2 = B(h\nu - E_g) \ldots\ldots (1)$$

Where B is a constant and α represents the absorption coefficient. As shown in Figure 6(b), the Tauc plot illustrates the optical band gap. The observed reduction in the band gap from 3.51 to 3.39 eV may be attributed to the incorporation of Zn, which introduces additional energy levels within the forbidden gap near the valence band, thereby narrowing the band gap.[16].

DOI:https://doi.org/10.25130/tjps.v31i3.1930

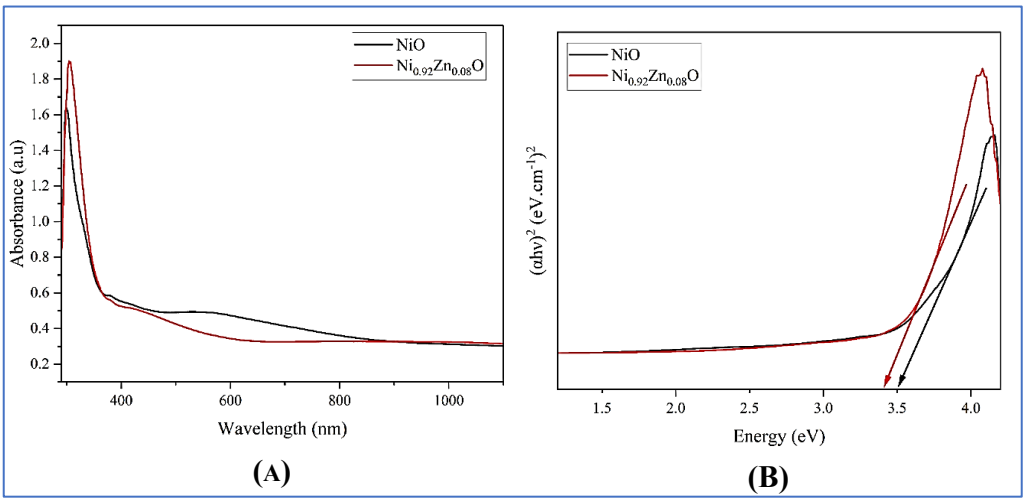

Fig. 6: (a) Absorbance as a function of wavelength, (b) Tauc plot of prepared thin films.

The Kramers-Kronig method is one of the most significant and precise approaches for extracting optical constants, such as the refractive index and extinction coefficient, from reflectance data as a function of angular frequency. $R(\omega)$. The following expression gives the complex refractive index. [17]:

$$\tilde{n} = n(\omega) + i\kappa(\omega) \ldots\ldots (2)$$

According to the K-K relations, the real part of the refractive index $n(\omega)$, which represents the reduction in the phase velocity of light entering the material, is given by the following equation.

$$n(\omega) = \frac{1-R(\omega)}{1+R(\omega)-2cos\delta(\omega)\sqrt{R(\omega)}} \ldots\ldots (3)$$

Meanwhile, the imaginary part $\kappa(\omega)$, which corresponds to the optical loss of light within the material, is expressed as follows [18, 19]:

$$\kappa(\omega) = \frac{1-R(\omega)sin\delta(\omega)}{1+R(\omega)-2cos\delta(\omega)\sqrt{R(\omega)}} \ldots\ldots (4)$$

where $\delta(\omega)$ represents the phase shift angle between the incident and reflected light and is calculated using the following equation [8, 17].

$$\delta(\omega) = -\left(\frac{\omega}{\pi}\right)\int_0^{\infty} \frac{lnR(\omega')-lnR(\omega)}{\omega'^2-\omega^2} d\omega' \ldots\ldots (5)$$

where the calculations were performed numerically using MATLAB (Figure 7), the refractive index of the prepared films is presented as a function of wavelength. The refractive index of NiO thin films varies depending on the preparation method and the film's structural characteristics. From the figure, it is observed that the refractive index increases with wavelength from 340 nm to approximately 750 nm, then stabilizes and gradually decreases at higher wavelengths. This behavior aligns with the refractive index trend described in the model proposed by [20].

Moreover, the refractive index at a wavelength of 630 nm is found to be 2.52 for the pristine film and 2.57 for the Zn-incorporated thin film. The increase in the refractive index observed in the doped film may be attributed to the enhanced optical polarizability resulting from the additional charge carriers introduced by Zn impurities. Additionally, an increase in film density could contribute to the same effect. [9].

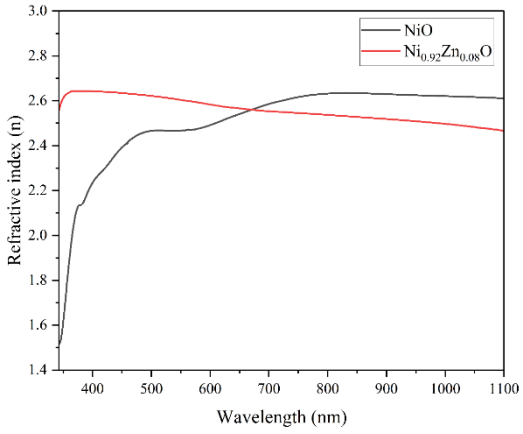

Fig. 7: Refraction indices by K-K calculations of the prepared thin films.

Similarly, Figure 8 shows the extinction coefficient as a function of wavelength, corresponding to the imaginary part of the complex refractive index. The figure shows a decrease in the extinction

DOI:https://doi.org/10.25130/tjps.v31i3.1930

coefficient with increasing wavelength for the NiO film. Additionally, the Ni0.92Zn0.08O film exhibits a significant reduction in the extinction coefficient, approaching zero at 372 nm, enabling greater light transmission.

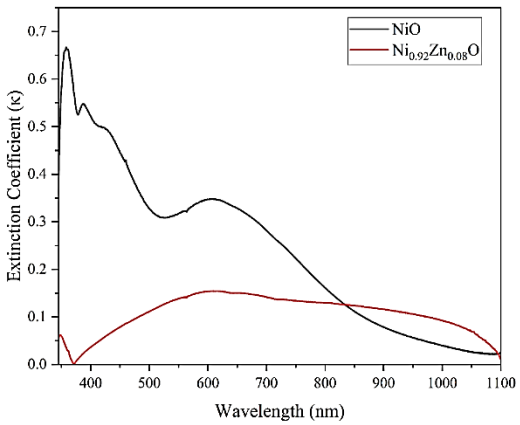

Fig. 8: The extinction coefficient as a function of wavelength.

After determining n and κ, the optical dielectric constant can be evaluated in terms of its real ε_1 and imaginary ε_2 components, offering insight into the optical behavior of the prepared films. These components describe the material's polarizability and optical energy dissipation and are given by the following expressions. [21]:

$$\varepsilon_1 = n^2 - \kappa^2 \dots\dots (6)$$

$$\varepsilon_2 = 2n\kappa \dots\dots (7)$$

Figures (9 and 10) illustrate the behavior of the optical dielectric constant in the wavelength range of 350–1100 nm, presenting its real and imaginary components as a function of wavelength. The trend of the real part ε_1 closely follows that of the refractive index due to their relationship, as described by equation 6. Additionally, Figure 10 reveals that the loss factor ε_2 It is generally lower in the Zn-doped thin film than in the undoped counterpart. This trend is consistent with the observed decrease in the extinction coefficient. κ, which signifies a reduction in optical losses. The incorporation of Zn is likely to reduce the number of defect states. This also suggests improved surface quality and grain packing in the $Ni_{0.92}Zn_{0.08}O$ film, leading to reduced surface roughness and a smoother overall morphology, highlighting its potential for optical applications.

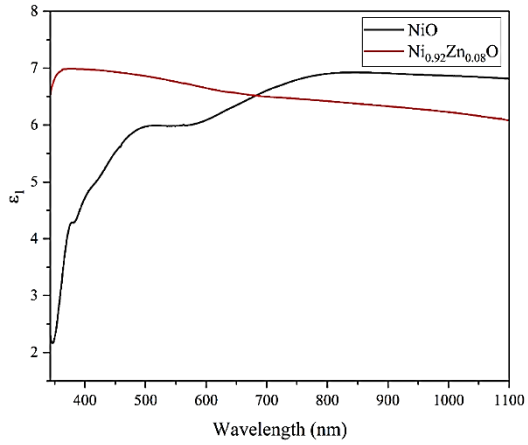

Fig. 9: Real part of optical dielectric constant.

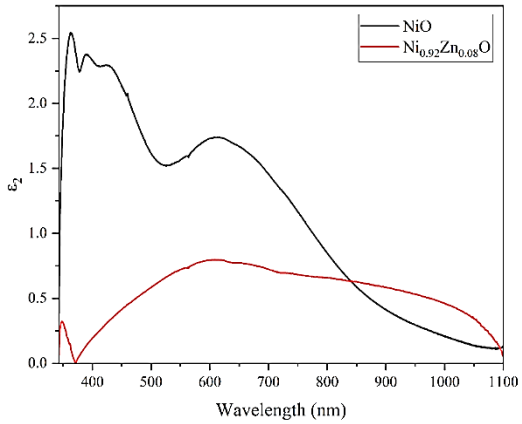

Fig. 10: Imaginary part of dielectric constant.

Table 1 provides a comparative analysis of E_g and n extracted in this study using Kramers-Kronig relations against values reported in the literature using different methods, offering insights into the consistency and validity of the obtained results.

DOI:https://doi.org/10.25130/tjps.v31i3.1930

Table 1: Some reported values of E_g and n.

Material	Bandgap (eV)	(630 nm)	Synthesis Method	Reference
NO	3.51	2.52	PLD	This Work
$Ni_{0.92}Zn_{0.08}O$	3.39	2.57	PLD	
$Ni_{1-x}Zn_xO$	3.25-3.49	Not reported	Chemical Spray Pyrolysis	(22)
$Ni_{1-x}Zn_xO$	3.76-3.93	2.66-2.87	Sol-gel spin coating	(23)
Zn-doped NiO nanoflake	3.61-3.67	2.33-2.34	Chemical Solution Deposition	(24)
NiO_x	3.64-3.85	2.36-2.39	DC magnetron sputtering	(25)
NiO/ITO	3.24	2.04	Electron beam deposition	(26)
NiO	3.05-3.1	Not reported	DC magnetron sputtering	(27)

CONCLUSION

In this study, NiO and $Ni_{0.92}Zn_{0.08}O$ thin films were synthesized using PLD in a vacuum onto glass substrates. XRD analysis was conducted to confirm the crystallinity of the prepared films, while their surface morphology was examined using FESEM. The incorporation of 8at. % Zn induced noticeable changes in the X-ray diffraction pattern, indicating modifications in the structural parameters due to Zn incorporation. Additionally, EDX confirmed the absence of impurities in the samples. The Tauc model was used to determine the optical bandgap, and the optical constants were extracted from reflectance data using the Kramers-Kronig (K-K) relations obtained with a UV-Vis-NIR spectrophotometer. The phase shift angle was numerically computed using MATLAB coding. The optical analysis revealed variations in the bandgap energy and optical constants between the two films. The bandgap decreased with Zn doping, and notable differences in the refractive index and dielectric behavior were observed between the two films, suggesting that Zn incorporation alters the electronic structure and transition probabilities. These findings underscore the effectiveness of the K-K method in accurately retrieving optical constants. Moreover, the results suggest that the optical properties of NiO thin films can be tailored through Zn doping, making these films promising candidates for optical and optoelectronic applications.

Conflict of interest: The authors declared no conflicts of interest.

Sources of funding: This research did not receive any specific grant from funding agencies in the public, commercial, or not-for-profit sectors.

Author contributions: The authors contributed equally to the study.

REFERENCE

1. Ukoba K, Eloka-Eboka A, Inambao F. Review of nanostructured NiO thin film deposition using the spray pyrolysis technique. Renewable and Sustainable Energy Reviews. 2018;82:2900-15. https://doi.org/10.1016/j.rser.2017.10.041

2. Benseghier SA, Bennabi F, Ercan I, Nehmar H, Khane Y, Moulayat N, et al. Low-Cost synthesis of Ag-doped NiO thin Films: Their structural, optical, photocatalytic and antimicrobial properties. Inorganic Chemistry Communications. 2024;159:111787. https://doi.org/10.1016/J.INOCHE.2023.111787

3. Aftab M, Butt M, Ali D, Bashir F, Khan TM. Optical and electrical properties of NiO and Cu-doped NiO thin films synthesized by spray pyrolysis. Optical Materials. 2021;119:111369. https://doi.org/10.1016/J.OPTMAT.2021.111369

4. Zhang J, Li W, Hoye R, MacManus-Driscoll J, Budde M, Bierwagen O, et al. Electronic and transport properties of Li-doped NiO epitaxial thin films .Journal of Materials Chemistry C. 2018;6(9):2275-82. https://doi.org/10.1039/C7TC05331B

5. Nandy S, Maiti U, Ghosh C, Chattopadhyay K. Enhanced p-type conductivity and band gap narrowing in heavily Al-doped NiO thin films deposited by RF magnetron sputtering. Journal of Physics: Condensed Matter. 2009;21(11):115804. https://doi.org/10.1088/0953-8984/21/11/115804

6. Kim KH, Kahuku M, Abe Y, Kawamura M, Kiba T. Improved electrochromic performance in nickel oxide thin film by Zn doping. International Journal of Electrochemical Science. 2020;15(5):4065-71. https://doi.org/10.20964/2020.05.28

7. Haider AJ, Alawsi T, Haider MJ ,Taha BA, Marhoon HA. A comprehensive review on pulsed laser deposition technique to effective nanostructure production: Trends and challenges. Optical and Quantum Electronics. 2022;54(8):488. https://doi.org/10.1007/s11082-022-03786-6

8. Ali HE, Ganesh V, Haritha L, Aboraia A, Hegazy H, Butova V ,et al. Kramers-Kronig analysis of the optical linearity and nonlinearity of nanostructured Ga-doped ZnO thin films. Optics & Laser Technology. 2021;135:106691. https://doi.org/10.1016/J.OPTLASTEC.2020.106691

9. Ganesh V, Haritha L, Ali HE, Aboraia A, Khairy Y, Hegazy H, et al. The detailed calculations of optical properties of indium-doped CdO nanostructured films using Kramers-Kronig relations. Journal of Non-Crystalline Solids. 2021;552:120454. https://doi.org/10.1016/J.JNONCRYSOL.2020.120454

10. Sharma R, Acharya A, Shrivastava S, Patidar MM, Gangrade M, Shripathi T, et al. Studies on the structural, optical and electrical properties of Zn-doped NiO thin films grown by spray pyrolysis. Optik. 2016;127(11):4661-8. https://doi.org/10.1016/J.IJLEO.2016.01.050

11. Ali A, Ahmad S, Usman M, Khan N, Hashim M, Ali Y, et al. Synthesis, characterization, optical and dielectric properties of NiO and Zn-doped NiO nanostructures: toward advanced applications. Advances in Condensed Matter Physics. 2024;2024(1):6645827. https://doi.org/10.1155/2024/6645827

12. Smal I, Yu Q, Veneman R, Fränzel-Luiten B, Brilman DWF. TG-FTIR Measurement of CO2-H2O co-adsorption for CO2 air capture sorbent screening. Energy procedia. 2014;63:6834-41. https://doi.org/10.1016/J.EGYPRO.2014.11.717

13. Arif M, Sanger A, Shkir M, Singh A, Katiyar R. Influence of interparticle interaction on the structural, optical and magnetic properties of NiO nanoparticles. Physica B: Condensed Matter. 2019;552:88-95. https://doi.org/10.1016/j.physb.2018.09.023

14. Sen T, Biswas A, Rout TK, Thangavel R, Nair UG. Comparative study of morphological, optical and conductive properties between low and heavily zinc-doped nickel oxide thin films as hole-transporting material. Journal of Alloys and Compounds. 2021;889:161613. https://doi.org/10.1016/J.JALLCOM.2021.161613

15. Viezbicke BD, Patel S, Davis BE, Birnie III DP. Evaluation of the Tauc method for optical absorption edge determination: ZnO thin films as a model system. Physica Status Solidi (b). 2015;252(8):1700-10. https://doi.org/10.1002/pssb.201552007

16. Ahamed NN, Pattar J, Kumar MA, Basavaraju N ,Raghavendra N, TM S, et al. Electrochemical studies of Zn-doped nickel oxide nanoparticles synthesized via the solution combustion method using green and chemical fuels. RSC advances. 2024;14(25):17664-74. https://doi.org/10.1039/D4RA01706D

17. Nazari N, Golzan M, Mabhouti K. Study of Urbach energy and Kramers–Kronig on Mn and Zn doped NiFe2O4 ferrite nanopowder for the determination of structural and optical characteristics. Scientific Reports. 2024;14(1):6407. https://doi.org/10.1038/s41598-024-57045-7

18. Aghgonbad MM, Sedghi H. Optical and electronic analysis of pure and Fe-doped ZnO thin films using spectroscopic ellipsometry and

Kramers–Kronig method. International Journal of Nanoscience. 2019;18(01):1850013. https://doi.org/10.1142/S0219581X18500138

19. Zak AK, Ghanbari A, ShekoftehNarm T. The effect of molybdenum on the optical properties of ZnO nanoparticles in the Ultraviolet–Visible region. Advanced Powder Technology. 2017;28(11):2980-6. https://doi.org/10.1016/J.APT.2017.09.006

20. Franta D, Negulescu B, Thomas L, Dahoo PR, Guyot M, Ohlídal I, et al. Optical properties of NiO thin films prepared by pulsed laser deposition technique. Applied surface science. 2005-1)244 .30-426:(4. https://doi.org/10.1016/J.APSUSC.2004.09.150

21. Dahham NA. Study of the Optical properties of CdS before and after irradiation by a CO2 laser for different exposure times. Tikrit Journal of Pure Science. 2015;20(2):171-6. https://doi.org/10.25130/tjps.v20i2.1177

22. Pothukanuri N, Reddy MR. Studies on pure and Zn-doped NiO nanostructured thin films for enhanced ammonia gas sensing applications. Chemical Physics Impact. 2024;8:100397. https://doi.org/10.1016/J.CHPHI.2023.100397

23. Benhamida S, Gouamid M, Tlili S, Khenblouche A, Charradi K. Structural, optical and dielectric properties of Zn-doped NiO thin films synthesized via sol-gel route. Dig J Nanomater Biostruct. 2021;16:433-42. https://doi.org/10.15251/DJNB.2021.162.433

24. Mamat M, Parimon N, Ismail A, Banu IS, Basha SS, Rani R, et al. Synthesis, structural and optical properties of mesostructured, X-doped NiO (x= Zn, Sn, Fe) nanoflake network films. Materials Research Bulletin. 2020;127:110860. https://doi.org/10.1016/J.MATERRESBULL.2020.110860

25. AF Lahiji F, Bairagi S, Magnusson R, Sortica MA, Primetzhofer D, Ekström E, et al. Growth and optical properties of NiO thin films deposited by pulsed DC reactive magnetron sputtering. Journal of Vacuum Science & Technology A. 2023;41.(6). https://doi.org/10.1116/6.0002914

26. Emam-Ismail M, El-Hagary M, El-Sherif H, El-Naggar A, El-Nahass M. Spectroscopic ellipsometry and morphological studies of nanocrystalline NiO and NiO/ITO thin films deposited by e-beam technique. Optical materials . .112:110763;2021 https://doi.org/10.1016/J.OPTMAT.2020.110763

27. Mustafa M, Ali M, Abdel-Wahab MS, Tawfik WZ, Eissa M, Elfayoumi M, et al. Using femtosecond laser pulses to investigate the thickness-dependent nonlinear optical properties of nickel oxide thin films and their potential use as optical limiters. Applied Optics. 2025;64(9):C1-C10. https://doi.org/10.1364/AO.532434